nature chemistry

ARTICLES

PUBLISHED ONLINE: XX XX 2017 | DOI: 10.1038/NCHEM.2877

Predicting DNA hybridization kinetics from sequence

Q1 Jinny X. Zhang[1,2], John Z. Fang[1], Wei Duan[1], Lucia R. Wu[1], Angela W. Zhang[1], Neil Dalchau[3], Boyan Yordanov[3], Rasmus Petersen[3], Andrew Phillips[3] and David Yu Zhang[1,2]*

Hybridization is a key molecular process in biology and biotechnology, but to date there is no predictive model for accurately determining hybridization rate constants based on sequence information. Here, we report a weighted neighbour voting (WNV) prediction algorithm, in which the hybridization rate constant of an unknown sequence is predicted based on similarity reactions with known rate constants. To construct this algorithm we first performed 210 fluorescence kinetics experiments to observe the hybridization kinetics of 100 different DNA target and probe pairs (36 nt sub-sequences of the CYCS and VEGF genes) at temperatures ranging from 28 to 55 °C. Automated feature selection and weighting optimization resulted in a final six-feature WNV model, which can predict hybridization rate constants of new sequences to within a factor of 3 with ~91% accuracy, based on leave-one-out cross-validation. Accurate prediction of hybridization kinetics allows the design of efficient probe sequences for genomics research.

Hybridization of complementary DNA and RNA sequences is a fundamental molecular mechanism that underlies both biological processes[1–3] and nucleic acid analytic biotechnologies[4–7]. The thermodynamics of hybridization have been well studied, and algorithms based on the nearest-neighbour model of base stacking[8,9] predict minimum free-energy structures and melting temperatures[10,11] with reasonably good accuracy. In contrast, the kinetics of hybridization remain poorly understood, and no models or algorithms have been reported that accurately predict hybridization rate constants from sequence and reaction conditions (temperature and salinity). This knowledge deficiency has adversely impacted the research community by requiring either trial-and-error optimization of DNA primer and probe sequences for new genetic regions of interest, or brute-force use of thousands of DNA probes for target enrichment.

Predictive modelling of hybridization kinetics faces two main challenges. First, the kinetics of very few DNA sequences have been characterized directly, either in bulk solution[12–16] or at the single-molecule level[17–19]. The primary reason for the lack of data is the cost of fluorophore-functionalized DNA oligonucleotides, which at roughly $200 per sequence becomes prohibitive for the hundreds of experiments needed to establish sequence generality. Second, the hybridization of complementary sequences can follow many different pathways[15], rendering simple reaction models inaccurate for a large fraction of DNA sequences.

To create a sufficiently representative and sequence-general data set for developing a predictive model of hybridization kinetics, we experimentally characterized the kinetics of 210 individual hybridization reactions on 100 different pairs of complementary sequences. We were able to do this economically through the use of the X-probe architecture, in which universal fluorophore- and quencher-functionalized oligonucleotides are recycled across many different experiments.

From our experimental data we made three unexpected findings: (1) most hybridization reactions do not asymptotically reach more than 90% yield; (2) initial hybridization kinetics is generally uncorrelated with asymptotic yield; and (3) secondary structure in the middle of a DNA target sequence tends to more adversely affect hybridization kinetics. Additionally, we observed that structure-free DNA target/probe sequences generally tended to have faster hybridization kinetics, consistent with literature and our expectations, but even structure-free sequences exhibited more than one order of magnitude of variation in hybridization rate constants.

Based on our experimental data, we also constructed a new type of algorithm to predict DNA hybridization rate constants based on the target/probe sequence, called 'weighted neighbour voting' (WNV). In WNV, each hybridization reaction is mapped to a set of bioinformatic feature values and can be considered a point in the high-dimensional feature space. Two hybridization reactions that are close in feature space are expected to exhibit similar kinetics. The rate constant of an unknown hybridization reaction is predicted based on the weighted average of observed rate constants of experimentally tested reactions, with weights dropping exponentially for reactions that are farther away in feature space. Under leave-one-out (LOO) cross-validation, our final WNV model predicts rate constants to within a factor of 2 for 80% of reactions, and within a factor of 3 for 91%. Next-generation sequencing (NGS) studies show a significant correlation ($R^2 \approx 0.6$) between the rate constants of DNA hybridization in single-plex versus multiplex, suggesting that the current work is a good starting point for the rational design and selection of DNA probes for highly multiplexed applications, such as target enrichment from genomic DNA[6].

Experimental results

To systematically but economically characterize the hybridization kinetics of many different sequences we used the X-Probe architecture[20], which makes use of universal fluorophore and quencher-labelled oligonucleotides (Fig. 1a). A universal fluorophore-labelled oligonucleotide was pre-hybridized to the probe and a universal quencher-labelled oligonucleotide was pre-hybridized to the target. When the target and probe solutions were mixed, the Q2

[1]Department of Bioengineering, Rice University, Houston, Texas 77030, USA. [2]Systems, Synthetic, and Physical Biology, Rice University, Houston, Texas 77030, USA. [3]Microsoft Research, Cambridge CB1 2FB, UK. *e-mail: dyz1@rice.edu

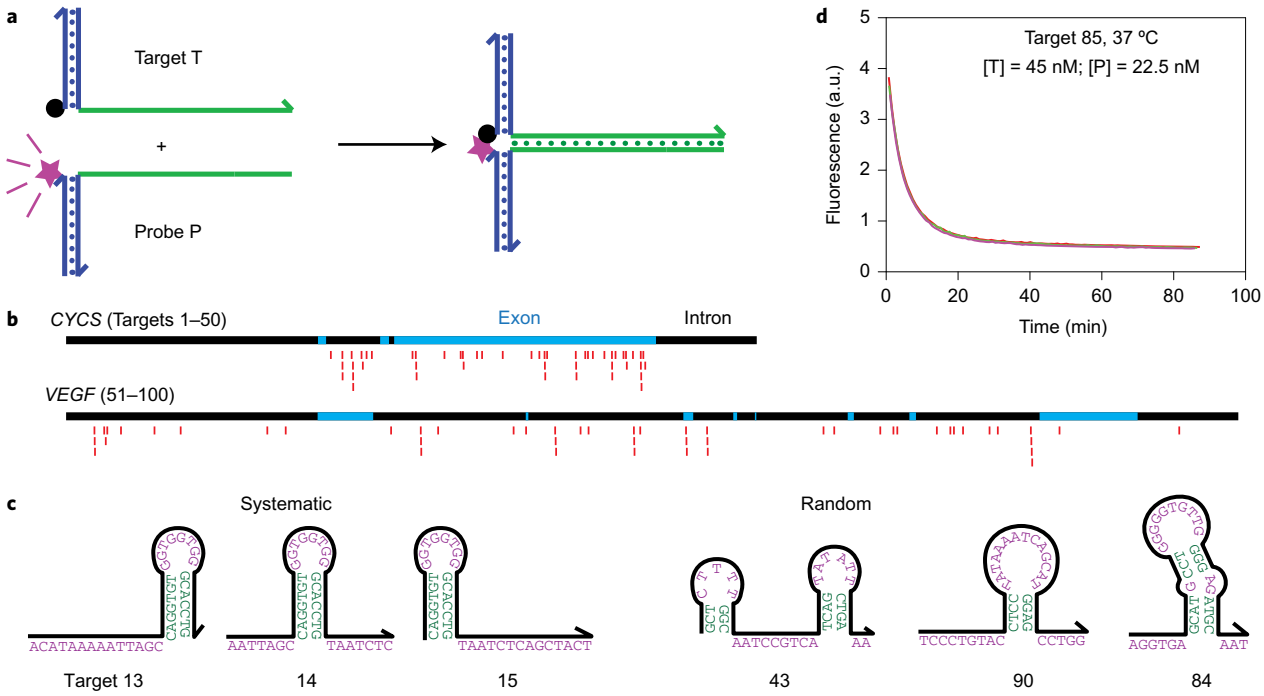

Figure 1 | Experimental characterization of hybridization kinetics. a, Fluorescent probes with universal functionalized oligonucleotides. Blue regions are universal sequences and green regions are variable regions corresponding to the target or probe sequence. Fluorescence is initially high and decreases as the hybridization reaction proceeds because the fluorophore (purple star) becomes localized to the quencher (black dot). **b**, A total of 100 different sub-sequences of the *CYCS* and *VEGF* genes were selected to be the target sequences. In this study, all target and probe sequences are 36 nt long (excluding universal regions). Then, 25 targets for each gene were chosen randomly with uniform distribution across the entire intron and exon region and another 25 targets were selected as close overlapping frames to systematically test the position effects of secondary structures. Red markers denote the sub-sequences of the genes selected as targets. **c**, Examples of secondary structures encountered in target sequences. Shown are predicted minimum free energy (mfe) structures predicted for the target sequences at 37 °C. Supplementary Table 1 presents the sequences of the 100 targets. **d**, Example kinetics traces (triplicate) of a hybridization reaction. All reactions proceeded in 5× PBS buffer. Supplementary Section 1 provides reproducibility studies and Supplementary Section 2 fluorescence traces for all 210 experiments.

solution fluorescence was initially high because the fluorophore was delocalized from the quencher, but dropped over time as the hybridization reaction proceeded. The solution fluorescence at any given time can thus be linearly mapped to the instantaneous hybridization reaction yield.

We selected, as targets, 100 sub-sequences of the *CYCS* and *VEGF* genes, each target sub-sequence being 36 nucleotides (nt) long. Of the 50 targets for each gene, 25 were selected randomly with uniform position distribution across the gene and the other 25 were selected systematically so that the effects of secondary structure position could be examined (Fig. 1b,c).

Figure 1d shows triplicate kinetics traces for one hybridization reaction. A total of 210 hybridization experiments were characterized (100 reactions at 37 °C, 96 at 55 °C, 7 at 28 °C and 7 at 46 °C). There was very low experimental error in our fluorescence experiments; all triplicate data points agreed with each other to within 2%. To obtain maximally reliable experimental data for rate constant inference, we performed multiple experiments until determining a set of target and probe concentrations such that each hybridization reaction undergoes between two and ten half-lives within the 80–180 min observation time.

In all experiments, the concentration of the target was at least double that of the probe, to minimize the effects of slight pipetting variability. To ensure that the observed kinetics are primarily due to target/probe sequence rather than synthesis impurities, we experimentally observed kinetics for the hybridization of three sets of targets and probes, each as three separate syntheses from two different vendors (Integrated DNA Technologies and Sigma). The inferred hybridization rate constants for different syntheses showed minor variations, and were all consistent to within a factor of 2 (Supplementary Section 1).

Hybridization rate constant (k_{Hyb}) fitting

A simple two-state $T + P \rightarrow TP$ reaction model fails to reasonably fit the observed fluorescence kinetics. Notably, over 40% of the reactions asymptote to a final reaction yield of less than 85%, based on the positive control fluorescence where the target and probe are thermally annealed (Supplementary Section 1). We were surprised by the extent and reproducibility of the incomplete DNA hybridization yield, which may be due to misaligned hybridization or other nonspecific interactions between target and probe.

We considered three reaction models of hybridization to explain the kinetics data (Fig. 2a). Model H1 assumes that a fraction of the probes P are incapable of proper hybridization with target T or the accompanying fluorescence quenching. Model H2 assumes that all probe P is correctly synthesized, but that some fraction of the $T + P$ reaction undergoes an alternative pathway with rate constant k_1 to result in a state TP_{bad} with high fluorescence. This frustrated state, TP_{bad}, may represent states in which T and P are co-localized by misaligned base pairs. Model H3 is a combination of models H1 and H2, wherein there exists both a fraction of bad P as well as the alternative pathway involving TP_{bad}.

For each of our 210 fluorescence kinetics experiments we performed fitting using each of the three models (Fig. 2b), finding parameters that minimize the sum-of-square relative error RE, where RE = ((Data – Simulation)/Data). The RE values of each hybridization experiment are summarized as a single root-mean-square

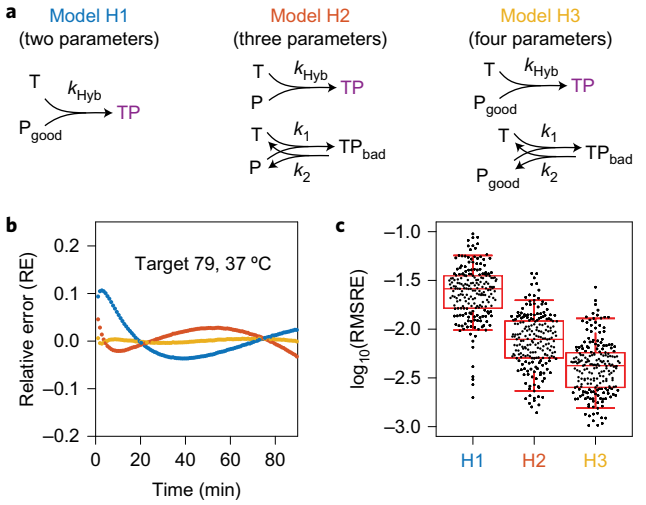

Figure 2 | Hybridization model and rate constant parameterization. **a**, Three different reaction models considered for fitting rate constant k_{Hyb} to fluorescence kinetics data. Based on the root-mean-square relative error (RMSRE) of each of the models in fitting the observed experimental data, model H3 was selected. Model 3 has four fitting parameters for each reaction: k_{Hyb}, bad fraction $(1-([P_{good}]/[P]))$, k_1 and k_2. **b**, Relative error (RE) for three reaction models for a given hybridization reaction. RE is plotted as a function of time for each model using best-fit parameters for each. **c**, Summary of fit quality for the three models across all 210 fluorescence kinetics experiments. Each point corresponds to the RMSRE of all time points for a particular fluorescence experiment. Upper and lower bars are 95th and 5th percentile values, and the box shows 75th, 50th and 25th percentile values. Based on this result, we chose to proceed with model H3 for all subsequent studies.

relative error (RMSRE) value, defined as

$$RMSRE = \sqrt{\frac{1}{\alpha}\sum_{t} \mathrm{RE}(t)^2}\# \quad (1)$$

where α is the total number of time points t during which fluorescence was measured for the reaction. Figure 2c shows the distribution of RMSRE values. Model H3 yields the best overall fit to the experimental data. Consequently, H3-fitted parameters (k_{Hyb} and the bad fraction) were used for all subsequent work. See Supplementary Section 2 for best-fit traces using each reaction model.

Summary of observed hybridization kinetics. The best-fit values of the hybridization rate constant k_{Hyb} at 37 and 55 °C are summarized in Fig. 3a. The observed k_{Hyb} ranged from 3.2 log at 37 °C and 2.3 log at 55 °C, significantly exceeding our expectations. Hybridization kinetics are generally faster at 55 °C than at 37 °C (by a factor of 3 on average), and there is a reasonably strong correlation between hybridization rate constants for the same target/probe pair at different temperatures.

The asymptotic yield of the fast initial hybridization reaction with rate constant k_{Hyb} can be quantitated as (1 – bad fraction). The bad fraction varies between 0.02 and 0.41 (Fig. 3b), and only appears to be marginally smaller on average at 55 °C than at 37 °C. Surprisingly, there are many cases (30 of 96) where the bad fraction is larger at 55 °C than at 37 °C. Because aliquots of the same DNA oligonucleotide molecules were used for both sets of experiments, it is not clear why such inversions are so common. There does not appear to be significant correlation between k_{Hyb} values and the bad fraction (Fig. 3c).

We next examined the systematically designed DNA target/probe sequence pairs for trends in k_{Hyb} (Fig. 3d). The systematic sequences included 13 sets of three DNA target/probe pairs, each frame-shifted a small number of bases so that predicted secondary structure lies in the 5′, middle or 3′ regions of the target (Fig. 1c). We observed two interesting trends. First, the observed k_{Hyb} values can vary greatly within a cluster: for example, targets 1–3 shows about 30-fold difference in hybridization rate constant, despite all three having similar standard free energies of folding. This indicates that the relative position of secondary structures within a DNA sequence can have a large impact on kinetics. Second, targets with the secondary structure in the middle of the sequence (circles in Fig. 3d) tended to be slower to hybridize than targets with the structure at one end: in 8 of the 13 clusters, the target with central secondary structure was the slowest in each respective cluster.

Literature reports[21] and our own prior experience suggested that unstructured DNA sequences would hybridize more rapidly and with higher yield than structured ones. To see whether our experimental data are consistent with this observation, we plotted k_{Hyb} and the bad fraction for only the hybridization reactions in which both the target and the probe have an ensemble (partition function) standard free energy $\Delta G°$ of >-3 kcal mol^{-1}, as predicted by Nupack[11] for hybridization temperature and buffer conditions (Fig. 3e,f). The observed k_{Hyb} values for these structure-free sequences are indeed faster than 'typical' sequences, with all k_{Hyb} $>1\times10^6$ M^{-1} s^{-1}. Nonetheless, there is still significant variability in k_{Hyb}, ranging over more than 1 log. The asymptotic yield of the hybridization reactions is only slightly better for structure-free sequences than for other sequences.

Predictive model construction

WNV model. Our WNV model predicts the value of k_{Hyb} for new hybridization reactions based on the similarity of the reaction to hybridization reactions with known rate constants (labelled instances). Each labelled instance makes a weighted vote of $\log_{10}(k_{Hyb})$, with instances that are more similar to the new reaction being weighted more heavily. The 210 hybridization reactions across 100 different target/probe pairs act as our initial database of labelled instances.

For each hybridization reaction, a number of features f_i are calculated based on the sequences of the target and probe and the hybridization reaction temperature and buffer (Fig. 4b). A total of more than 50 different features were tested, of which 35 showed significant individual correlation with k_{Hyb} (Supplementary Section 4). The disparity between two different hybridization reactions j and m is quantitated as distance $d_{j,m}$, the Euclidean distance between the two hybridization reactions in feature space:

$$d_{j,m} = \sqrt{\sum_i \left(f_i(j) - f_i(m)\right)^2}\# \quad (2)$$

where $f_i(j)$ is the value of weighted feature i for reaction j. Higher weights result in a wider feature dimension, which can potentially contribute more to the feature space distance (Fig. 4d).

From the database of hybridization experiments m with known $k_{Hyb}(m)$ values, our WNV model makes the following prediction for $k_{Hyb}(j)$ of an unknown hybridization reaction j:

$$\log_{10}\left(\hat{k}_{Hyb}(j)\right) = \frac{1}{Z_j}\sum_m 2^{-d_{j,m}} \log_{10}\left(k_{Hyb}(m)\right)\# \quad (3)$$

where $Z_j = \sum_m 2^{-d_{j,m}}$ is the 'partition function' of the distances involving reaction j (Fig. 4e). Figure 4f shows the relationship between feature space distance between a pair of hybridization

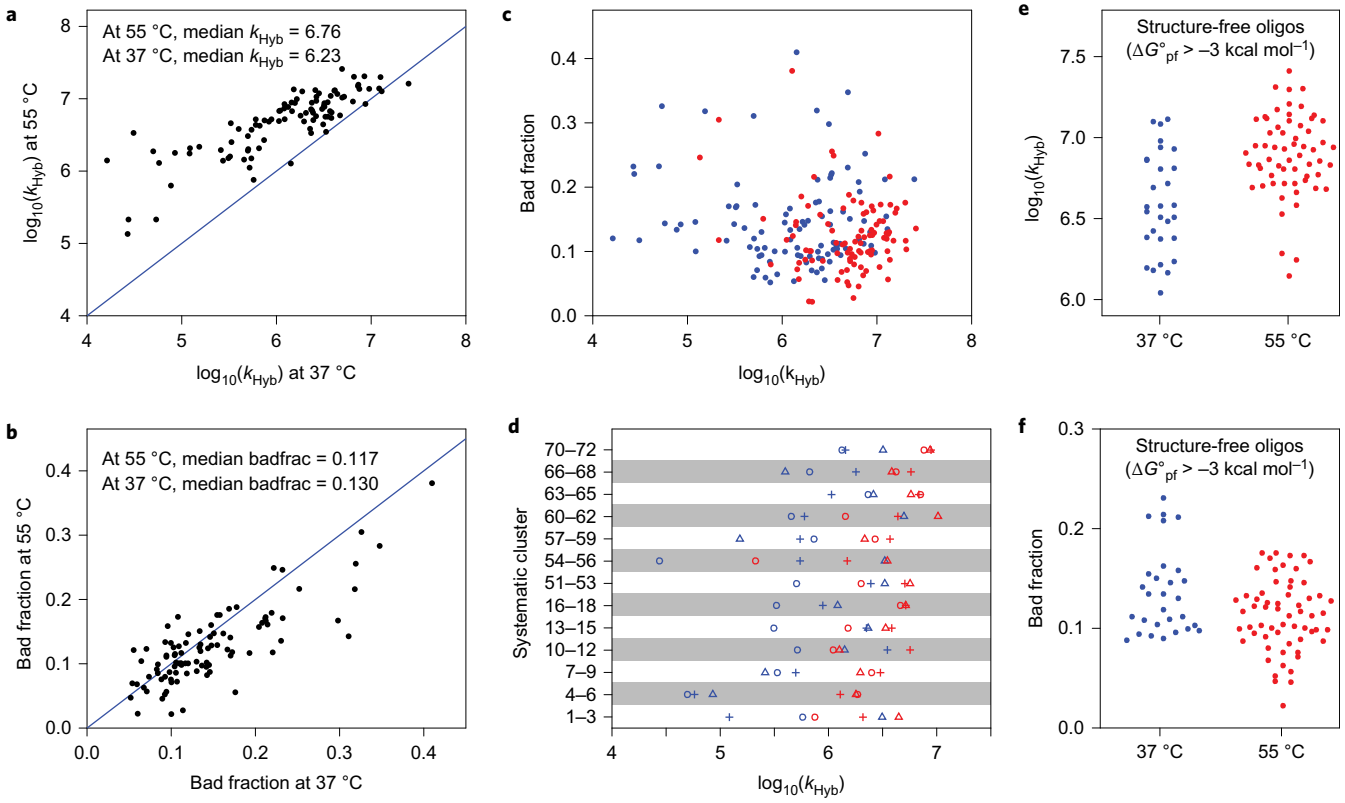

Figure 3 | Summary of observed hybridization kinetics. a, Observed k_{Hyb} value (model H3) for 96 targets at 37 and 55 °C. Four A/T targets were excluded from this because they were A/T-rich and did not stably bind to their probes at 55 °C. **b**, Most reactions did not reach completion, instead saturating at between 60 and 100% yield. Yield was determined based on positive control experiments where target and probe were thermally annealed (Supplementary Section 1). We modelled incompleteness of hybridization as a 'bad fraction' of probes that becomes kinetically trapped at a high fluorescence state. The best-fit bad fractions for the 96 targets at 37 and 55 °C are plotted. **c**, There appears to be no correlation between k_{Hyb} and asymptotic yield. Blue and red dots show experiments at 37 °C and at 55 °C, respectively. **d**, Systematically designed target/probe sequences included 13 clusters, each comprising three targets. Within each cluster, the target sequences were shifted such that predicted secondary structure is present (1) near the 5′ end (plus symbols), (2) near the middle (circles), or (3) near the 3′ end of the target (triangles). In 8 of 13 clusters, the target with structure in the middle was slowest. **e**, Because secondary structures are known to slow down kinetics[21], we examined the target/probe pairs in which both the target and the probe had a predicted ensemble (partition function) standard free energy ($\Delta G°_{pf}$) of greater than –3 kcal mol^{-1} at the experimental hybridization temperature, indicating minimal structure. At 37 °C and 55 °C, 29 of 100 reactions and 61 of 96 reactions satisfied this criterion, respectively. These reactions all have $k_{Hyb} \geq 1 \times 10^6$ M^{-1} s^{-1}, but k_{Hyb} values range over more than one order of magnitude. **f**, Minimal-structure targets exhibit significant variability of bad fraction, ranging between 0 and 25%.

reactions (using our final feature list and weights) and their difference in observed k_{Hyb} values.

The WNV model can be extended to any number of features. In general, the potential improvements in k_{Hyb} prediction accuracy must be balanced against increased model complexity from having a large number of features. Additionally, the higher-dimensional feature space that accompanies an increased number of features makes the weight optimization significantly more difficult, due to the increased number of local fitness maxima. Through a series of computational optimization steps, we determined the optimal number of features to be 6: nGp, Pap, Temp, wPat, GavgMSR1 and Gb (see Supplementary Section 3 for the optimization methodology).

Model performance. To quantitate the overall performance of a particular WNV model (defined by its set of features and corresponding feature weights $w(i)$), we constructed the following 'Badness' metric:

$$Badness = 3 \times (1 - \text{F2acc}) + 3 \times (1 - \text{F3acc}) + 4 \times RMSE\# \quad (4)$$

where F2acc is the fraction of all predicted reactions j in which the predicted $\hat{k}_{Hyb}(j)$ and the experimental $k_{Hyb}(j)$ agree to within a factor of 2, F3acc is the fraction that agrees to within a factor of 3, and

$$RMSE = \sqrt{\frac{1}{N}\sum_j \left(\log_{10}\left(k_{Hyb}(j)\right) - \log_{10}\left(\hat{k}_{Hyb}(j)\right)\right)^2}\# \quad (5)$$

is the root-mean-square error of the logarithm of the hybridization rate constant (where $N = 210$ is the number of experiments).

We chose to use this badness metric rather than RMSE only (that is, a least-squares fit) because we felt that it is more relevant for many applications involving the design of DNA oligonucleotide probes and primers. Rather than marginally improving the predictions of outlier sequences that are off by more than an order of magnitude, our badness metric instead emphasizes improving the fraction of predictions that are correct to within a factor of 3, or better yet within a factor of 2. Simultaneously, to allow efficient computational optimization of feature weights, the badness metric to be minimized cannot be locally flat, so RMSE is included as a component of badness. Use of different badness metrics will result in optimized feature weights that exhibit a different tradeoff between the magnitude and frequency of large prediction errors.

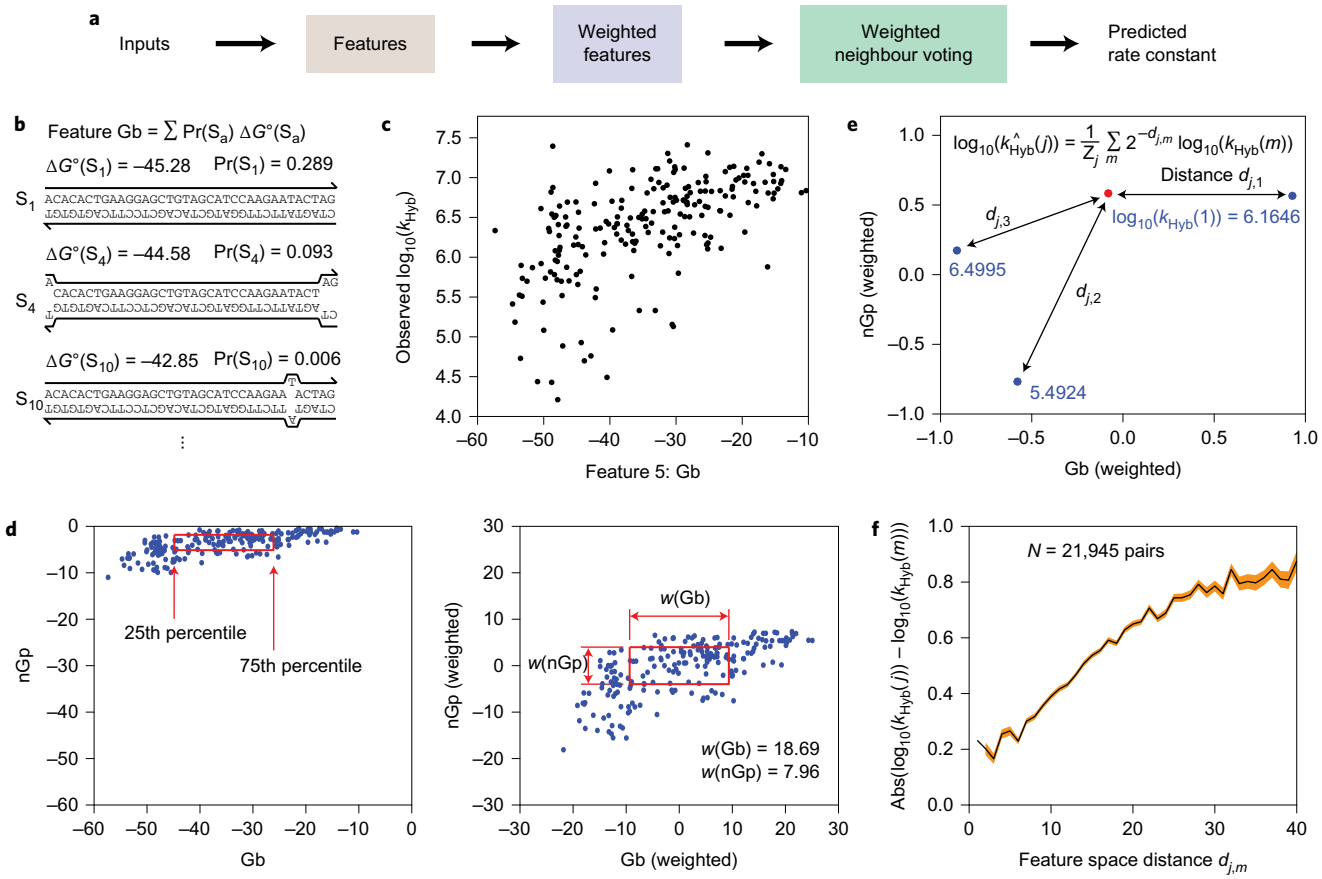

Figure 4 | Rate constant prediction using the WNV model. a, For an unknown hybridization reaction whose rate constant is to be predicted, feature values are calculated and compared to those in the database. The observed rate constants in the database are integrated via a weighted voting system, with weight decreasing exponentially based on distance to the target in feature space. **b**, Features are computed based on the sequences of the target and probe, as well as the reaction conditions (temperature, salinity). Shown is an example calculation for feature Gb, the weighted average $\Delta G°$ of the hybridized complex. **c**, Relationship between the experimental hybridization rate constants k_{Hyb} (in $\log_{10}$) versus Gb values for the 210 hybridization experiments. There is moderate correlation between k_{Hyb} and Gb, indicating that Gb may be an effective feature for rate constant prediction. **d**, Feature renormalization. Raw values of the Gb and nGp features (left) are linearly transformed based on a set of feature weights $w(i)$: the 75th percentile value of a feature i is renormalized to $+(w(i)/2)$ and the 25th percentile value is renormalized to $-(w(i)/2)$. **e**, The distance between renormalized feature values of an unknown reaction (red dot) and of all reactions with known k_{Hyb} values (blue dots) are computed. Prediction weight drops exponentially with distance. **f**, Relationship between feature space distance d and the absolute value of difference in experimental rate constants ($\log_{10}$) for two hybridization reactions. Pairs of reactions with small d generally have similar rate constants; the converse statement is not true because two very different reactions may coincidentally have similar rate constants. The black line shows the mean and the red region shows ±1 standard deviation on the mean.

One commonly held belief in the field is that the predicted secondary structure in the DNA target and probe sequences is highly inversely correlated with hybridization rate constants. We found this to be partially true: when the WNV model is constrained to the selection of only a single feature, the nGp feature (denoting the predicted $\Delta G°$ of the probe oligonucleotide based on Nupack at the hybridization temperature/buffer) emerged as the single best predictor of k_{Hyb} (Fig. 5a). Prediction using only nGp was accurate to within a factor of 2 for 61% of reactions and within a factor of 3 for 79% of reactions. However, prediction accuracy can be significantly improved by including more features in the WNV model.

Figure 5b,c shows the prediction accuracy of the best three-feature WNV model and the final six-feature WNV model. The six-feature WNV model is significantly better at prediction than the one-feature and three-feature models, with 80% accuracy within a factor of 2 and 91% accuracy within a factor of 3. The six features used were nGp, Pap, Temp, wPat, GavgMSR1 and Gb, with respective feature weights of 7.96, 15.12, 10.55, 4.44, 10.90 and 18.69 (Supplementary Section 4). Although nGp was the best single feature when considered in isolation, in the six-feature model its weight is the second smallest. This observation potentially suggests that the other features collectively hold information that overlaps with nGp.

To help the research community predict hybridization rate constants for DNA oligo probes and primers, we have constructed a web-based software tool, available at http://nablab.rice.edu/nab-tools/kinetics. The software typically completes predicting k_{Hyb} within 30 s. It is currently seeded with the 210 hybridization experiment results performed in this Article and will be updated with additional hybridization experiment results in the future.

Enrichment from human genomic DNA

The human genome is over 3 billion nucleotides long, but the coding regions that form the exome collectively only span 1% of the genome. Within the 20,000 genes of the exome, typically there are only between 10 and 400 that are relevant to any particular disease. NGS[22,23] is the preferred way to perform highly multiplexed analysis of many different DNA sequences within a sample. In NGS, anywhere between 1 million and 1 billion molecules are randomly sampled and the identities of the first 150–300 nt of each molecule

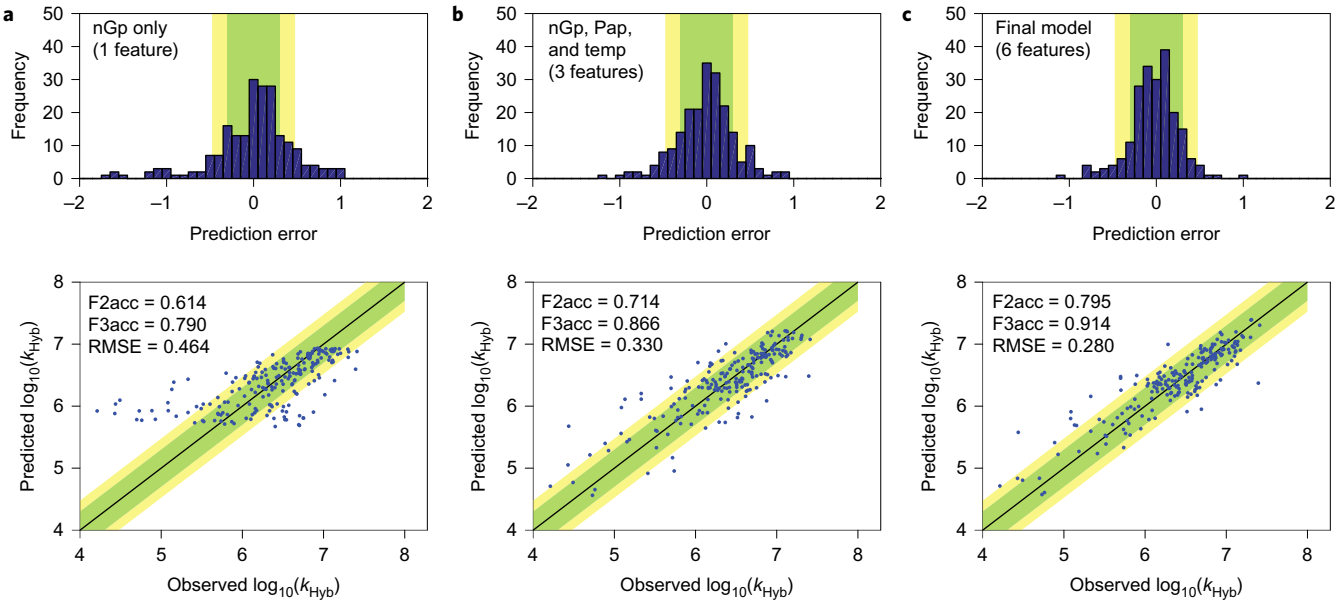

Figure 5 | Prediction accuracy of the WNV model using different numbers of features. a, Prediction using a single feature, nGp, denoting the ensemble (partition function) standard free energy of the probe, as predicted by Nupack[11] under the reaction conditions of interest. Top: Distribution of prediction error for k_{Hyb} (in $\log_{10}$). Bottom: Predicted vs observed k_{Hyb} values. Each blue dot plots the predicted $\log_{10}(\hat{k}_{Hyb})$ value versus the experimentally observed $\log_{10}(k_{Hyb})$ value for a single hybridization experiment. Each prediction was performed using a standard leave-one-out (LOO) approach: each k_{Hyb} prediction is based on 209 labelled instances (all reactions except the one to be predicted). The feature weights trained on all 210 data points (see Supplementary Section 3 for more details). **b**, Prediction using a three-feature WNV model, including nGp, Pap and temperature. **c**, Prediction using the final six-feature model.

are reported (subject to a sequencing error rate of between 0.1 and 1%); each reported sequence is known as a read. To observe potential variability in the DNA sequence at particular genomic regions, it is desirable to sample multiple molecules (high read depth). Solid-phase enrichment using highly multiplexed hybridization by synthetic DNA oligonucleotide probes[6] is often used for these targeted sequencing applications.

Current commercial multiplex hybrid-capture panels generally use a very large number of synthetic probe oligonucleotides to fully tile or overlap-tile the genomic regions of interest (for example, 200,000 probes for whole-exome enrichment). Due to the large number of oligo species involved, the concentration of each species is thus necessarily quite low (tens of picomolar), resulting in hybrid-capture protocols that typically last at least 4 h and more frequently more than 16 h. Because of the varying hybridization kinetics of different probes (Fig. 3d), it is likely that many probes do not contribute significantly to hybridization yield and in fact slow down the hybrid-capture process by forcing lower concentrations of the fast-hybridizing probes.

To experimentally test this possibility, we first applied our hybridization rate constant prediction algorithm to all possible 36 nt probes to exon regions of 21 genes. Because the exon regions are typically 3,000 nt long, this corresponds to roughly 3,000 possible probes per gene. Predicted rate constants typically range over about two orders of magnitude (Supplementary Fig. 5), with the fast (≥95th percentile) probes typically being a factor of 3 faster than median probes (~50th percentile). NGS hybrid-capture enrichment typically uses probes longer than 36 nt (for example, Agilent SureSelect uses 120 nt probes), but there is probably a similar if not greater range of hybridization rate constants for longer probes due to the greater possibility of secondary structure and nonspecific interactions.

Next, we picked a total of 65 fast probes and 65 median probes across the exon regions of 21 different cancer-related genes. The expectation was that after a 24 h hybridization protocol, the fast and median probes would produce similar reads, but with a short 20 min hybridization protocol, the fast probes would exhibit significantly greater reads than median probes (Fig. 6a). Our library preparation protocol is summarized in Fig. 6b. All 130 probes are hybridized to the adaptor-ligated DNA simultaneously. However, the number of reads aligned to a particular probe is not directly proportional to its hybridization yield, due to well-documented sequencing bias[24,25]. For example, some adaptor-ligated amplicons exhibit significant secondary structure and are less efficiently PCR-amplified during normalization, or less efficiently sequenced due to lower flow cell binding efficiency. For this reason, 15 fast and 15 median probes targeting four genes resulted in less than 100× sequencing depth and were excluded from subsequent analysis (Supplementary Section 5). We do not believe this affects the conclusions from our genomic DNA enrichment study.

Our comparison of reads for the 20 min hybridization library and the 24 h hybridization library indicates that the probes predicted to be fast on average exhibited both a twofold increase in reads in the 20 min library, and a twofold increase in the ratio of reads at 20 min versus 24 h. This is slightly worse than our algorithm's predicted threefold difference between median and fast probes, but understandable given that our rate constant prediction algorithm was trained on single-plex hybridization rather than on multiplex hybridization. Our calibration experiments (Supplementary Section 5) indicate that the correlation constant between single-plex and multiplex k_{Hyb} values is approximately $r^2 = 0.6$.

Our results thus suggest that sparse hybrid-capture enrichment panels would produce faster kinetics at a significantly lower cost. Rather than fully tiling or overlap-tiling the genetic regions of interest, it would be better to use a higher concentration of a few probes with the fastest hybridization kinetics. Multiple probes are only needed insofar as biological genomic DNA may be fragmented and a different probe is needed to capture each fragment. With the notable exception of cell-free DNA[26], most genomic DNA from clinical samples is longer than 500 nucleotides.

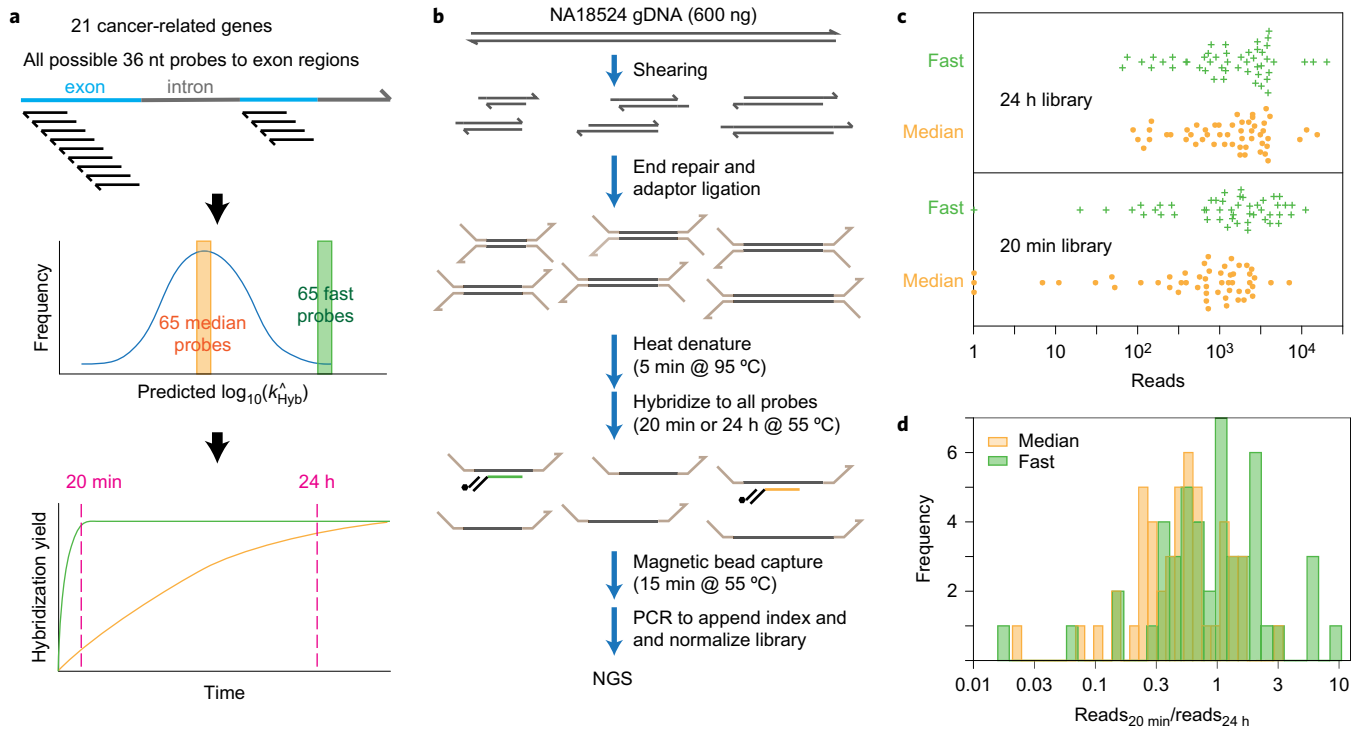

Figure 6 | Comparison of probes predicted to possess median vs fast hybridization kinetics for enrichment from human genomic DNA. a, Hybridization rate constants k_{Hyb} were predicted for all possible 36-mer hybridization probes for the exon regions of 21 cancer-related genes. The middle and lower panels express the idea behind probe selection and library design and do not accurately reflect kinetics distributions or trajectories of any particular gene or probe. See Supplementary Fig. 5 for the distribution of predicted k_{Hyb} for the *AQP1* gene. **b**, Genomic DNA enrichment and library preparation workflow. All hybridization probes were present at 50 pM concentration. See Methods for the detailed protocol. **c**, Bee swarm plot of NGS reads aligned to each probe, excluding 15 fast and 15 median probes to four genes with low read depth (Supplementary Section 5). In the library in which probes were hybridized to the fragmented gDNA for 24 h (top), there is no significant difference in the read count distribution between the median and fast probes. In the 20 min hybridization library, the fast probes showed significantly higher reads than the median probes, indicating that the probes our algorithm predicted to be faster did in fact provide a higher degree of hybridization within 20 min. **d**, Ratio of aligned reads in the 20 min library to those in the 24 h library for each probe. A high ratio indicates fast hybridization kinetics, and the ratio can exceed 1 because libraries were normalized, so fast probes are more dominant and occupy more reads in the 20 min library.

The concentrations of the probes used for this study were intentionally selected to be 50 pM per probe so as to be similar to probe concentrations in commercial enrichment kits. At 50 pM concentrations, up to 200,000 probes can be used and the total oligo concentration would still be at a reasonable 10 μM. At the significantly (for example, 10×) higher individual probe concentrations that become feasible with a sparse coverage of target genetic regions, even the 20 min allotted here for hybridization could be further reduced, greatly speeding up the enrichment workflow from the current practice of 4–24 h.

Discussion

Here, we have combined a rational design of features and the WNV framework with computational optimization of feature selection and feature weights, resulting in a final model that is capable of accurately predicting hybridization kinetics rate constants based on sequence and temperature information. The WNV model is highly scalable and easily incorporates new experimental data to provide improved predictions, without requiring model retraining. With every additional hybridization experiment and its accompanying fitted k_{Hyb} value, the six-dimensional feature space becomes denser, ensuring that on average a new hybridization experiment will be closer to an existing labelled instance.

To seed the model with a reliable initial database of labelled instances that is representative of the diversity of genomic DNA sequences, we experimentally characterized the kinetics of 210 hybridization experiments across 100 biological target sequences using fluorescence. The X-probe architecture allowed us to economically study kinetics for a reasonably large number of target sequences, but extra nucleotides of the universal arms may cause hybridization kinetics to differ slightly from that of a standard single-stranded probe. For example, there may be a systematic bias towards lower rate constants because of the reduced diffusion constants. Nonetheless, because all targets/probes use the same universal arm sequences, it is likely that the relative ordering of rate constants is preserved.

In this work we started with over 50 rationally designed features that we eventually pruned down to 6 in the final model. The high LOO validation accuracy of the WNV model indicates that these features capture a significant, if not majority, portion of the complexity of the hybridization process. Simultaneously, there remain pairs of experiments in our database with similar feature values but significantly different k_{Hyb} values. This implies the existence of undiscovered features that would distinguish these pairs of experiments; additional insight and creativity from the community in designing additional features would be welcomed.

The hybridization reactions experimentally characterized in the work were all performed in 5× PBS buffer and all target and probe sequences were 36 nt long. These experiment constraints were designed to reduce the diversity of hybridization reactions, to ease the training of the WNV model. We plan to expand our experimental studies to vary these conditions, to allow the WNV model to accurately account for buffer conditions and probe lengths. We suspect that longer DNA target/probe systems will exhibit even

more variability in hybridization kinetics; conversely, shorter DNA binding (for example, 10 nt) may exhibit less variability in k_{Hyb}. Additionally, with genomic DNA targets, the long-range secondary structure and the fragmentation pattern of genomic DNA targets should also be considered. New features will probably be needed for such expanded models.

Multiplex hybrid-capture panels for enriching target regions from genomic DNA are commonly used in targeted sequencing for scientific and clinical studies. In the absence of reliable kinetics prediction software, researchers and companies have taken a brute-force probe design approach, using fully tiled or overlapping-tiled probes to cover genetic loci of interest. Although this approach ensures the presence of at least some fast-binding probes, it is both expensive (in terms of synthesis and QC of thousands of probes) and results in slower workflows. Accurately predicting multiplexed hybridization kinetics will enable precision design of sparse, high-performance probe panels for target enrichment.

Data availability. Sequences used for all experiments are provided in the Supplementary Information. Raw fluorescence traces are plotted in the Supplementary Information and exact numerical data are available upon request. Calculated feature values are provided in the Supplementary Information.

Software availability. We have constructed a web-based software tool, available at http://nablab.rice.edu/nabtools/kinetics, that computes the predicted rate constant of a hybridization reaction given the sequence and temperature. The software typically completes the prediction of k_{Hyb} within 30 s. It is currently seeded with the 210 hybridization experiment results performed in this Article and will be updated with additional hybridization experiment results in the future.

Received 31 October 2016; accepted 21 September 2017; published online XX XX 2017

References

1. Hamilton, A. J. & Baulcombe, D. C. A species of small antisense RNA in posttranscriptional gene silencing in plants. *Science* **286,** 950–952 (1999).
2. Kornberg, A. & Baker, T. A. *DNA Replication* (Freeman, 1992).
3. Lewis, B. P., Burge, C. B. & Bartel, D. P. Conserved seed pairing, often flanked by adenosines, indicates that thousands of human genes are microRNA targets. *Cell* **120,** 15–20 (2005).
4. Izkoviz, S. & van Oudenaarden, A. Validating transcripts wih probes and imaging technology. *Nat. Methods* **8,** S12–S19 (2011).
5. Lockhart, D. J. *et al.* Expression monioring by hybridization to high-densiy oligonucleotide arrays. *Nat. Biotechnol.* **14,** 1675–1680 (1996).
6. Gnirke, A. *et al.* Solution hybrid selection wih ultra-long oligonucleotides for massively parallel targeted sequencing. *Nat. Biotechnol.* **27,** 182–189 (2009).
7. Khodakov, D., Wang, C. & Zhang, D. Y. Diagnostics based on nucleic acid sequence variant profiling: PCR, hybridization, and NGS approaches. *Adv. Drug Delivery Rev.* **105,** 3–19 (2016).
8. Mathews, D. H., Sabina, J., Zuker, M. & Turner, D. H. Expanded sequence dependence of thermodynamic parameters improves prediction of RNA secondary structure. *J. Mol. Biol.* **288,** 911–940 (1999).
9. SantaLucia, J. & Hicks, D. The thermodynamics of DNA structural motifs. *Ann. Rev. Biochem.* **33,** 415–440 (2004).
10. Zuker, M. Mfold web server for nucleic acid folding and hybridization prediction. *Nucleic Acids Res.* **31,** 3406–3415 (2003).
11. Zadeh, J. N. *et al.* NUPACK: analysis and design of nucleic acid systems. *J. Comput. Chem.* **32,** 170–173 (2011).
12. Morrison, L. E. & Stols, L. M. Sensitive fluorescence-based thermodynamic and kinetic measurements of DNA hybridization in solution. *Biochemistry* **32,** 3095–3104 (1993).
13. Reynaldo, L. P., Vologodskii, A. V., Neri, B. P. & Lyamichev, V. I. The kinetics of oligonucleotide replacements. *J. Mol. Biol.* **297,** 511–520 (2000).
14. Zhang, D. Y. & Winfree, E. Control of DNA strand displacement kinetics using toehold exchange. *J. Am. Chem. Soc.* **131,** 17303–17314 (2009).
15. Ouldridge, T. E., Šulc, P., Romano, F., Doye, J. P. K. & Louis, A. A. DNA hybridization kinetics: zippering, internal displacement and sequence dependence. *Nucleic Acids Res.* **41,** 8886–8895 (2013).
16. Schreck, J. S. *et al.* DNA hairpins destabilize duplexes primarily by promoting melting rather than by inhibiting hybridization. *Nucleic Acids Res.* **43,** 6181–6190 (2015).
17. Cisse, I. I., Kim, H. & Ha, T. A rule of seven in Watson–Crick base-pairing of mismatched sequences. *Nat. Struct. Mol. Biol.* **19,** 623–627 (2012).
18. Jungmann, R. *et al.* Single-molecule kinetics and super-resolution microscopy by fluorescence imaging of transient binding on DNA origami. *Nano Lett.* **10,** 4756–4761 (2010).
19. He, G., Li, J., Ci, H., Qi, C. & Guo, X. Direct measurement of single-molecule DNA hybridization dynamics with single-base resolution. *Angew. Chem. Int. Ed.* **55,** 9036–9040 (2016).
20. Wang, J. S. & Zhang, D. Y. Simulation-guided DNA probe design for consistently ultraspecific hybridization. *Nat. Chem.* **7,** 545–553 (2015).
21. Gao, Y., Wolf, L. K. & Georgiadis, R. M. Secondary structure effects on DNA hybridization kinetics: a solution versus surface comparison. *Nucleic Acids Res.* **34,** 3370–3377 (2006).
22. van Dijk, E. L., Auger, H., Jaszczyszyn, Y. & Thermes, C. Ten years of next-generation sequencing technology. *Trends Genet.* **30,** 418–426 (2014).
23. Koboldt, D. C., Steinberg, K. M., Larson, D. E., Wilson, R. K. & Mardis, E. R. The next-generation sequencing revolution and is impact on genomics. *Cell* **155,** 27–38 (2013).
24. Chilamakuri, C. S. *et al.* Performance comparison of four exome capture systems for deep sequencing. *BMC Genomics* **15,** 449 (2014).
25. Clark, M. J. *et al.* Performance comparison of exome DNA sequencing technologies. *Nat. Biotechnol.* **29,** 908–914 (2011).
26. Snyder, M. W., Kircher, M., Hill, A. J., Daza, R. M. & Shendure, J. Cell-free DNA comprises an *in vivo* nucleosome footprint that informs is tissues-of-origin. *Cell* **164,** 57–68 (2016).
27. Denoeux, T. A k-nearest neighbor classification rule based on Dempster–Shafer theory. *IEEE Trans. Syst. Man Cybern.* **25,** 804–813 (1995).
28. Wand, M. P. & Jones, M. C. *Kernel Smoothing* (CRC Press, 1994).

Acknowledgements

The authors thank S.X. Chen for assistance with NGS sequence alignment. This work was funded by National Institutes of Health grant R01HG008752 to D.Y.Z.

Author contributions

J.X.Z., L.R.W. and D.Y.Z. conceived the project. J.X.Z. and A.W.Z. performed the experiments. N.D. and A.P. performed hybridization reaction model fitting and selection. J.X.Z., J.Z.F., B.Y. and R.P. performed feature construction. W.D. and D.Y.Z. performed WNV model construction and optimization. N.D., B.Y. and R.P. performed MLR model construction and optimization. D.Y.Z. wrote the manuscript with input from all authors.

Additional information

Supplementary information is available in the online version of the paper. Reprints and permissions information is available online at www.nature.com/reprints. Publisher's note: Springer Nature remains neutral with regard to jurisdictional claims in published maps and institutional affiliations. Correspondence and requests for materials should be addressed to D.Y.Z.

Competing financial interests

There is a patent pending on the X-probes used in this work, and a patent pending on the WNV model of hybridization rate constant prediction.

nchem.2877 Table of Contents summary

The rate constant of DNA hybridization varies over several orders of magnitude and is affected by temperature and DNA sequence. A machine-learning algorithm that is capable of accurately predicting hybridization rate constants has now been developed. Tests with this algorithm showed that over 90% of predictions were correct to within a factor of three.

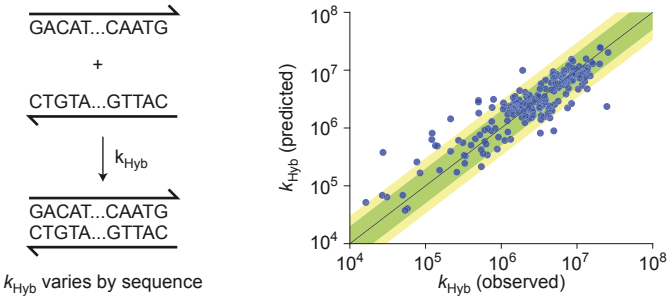

Journal: Nature Chemistry

Article ID: nchem.2877

Article title: Predicting DNA hybridization kinetics from sequence

Authors: Jinny X. Zhang *et al*.

AQ1	Author surnames have been highlighted - please check these carefully and indicate if any first names or surnames have been marked up incorrectly. Please note that this will affect indexing of your article, such as in PubMed.	
AQ2	Refs 20 and 21 were not cited in the text – we have reordered the citations and references in order of appearance in the text and these uncited references are now numbered 27 and 28. If you wish to retain them, please indicate where they should be mentioned in the text.	
AQ3	In equations (1) (2) etc., please clarify what # indicates. Should this be deleted throughout?	
AQ4	Please expand QC.	
AQ5	Can we be more specific here about where you mean in the Supplementary Information? Can we give a section number or title?	